J. Geogr. Sci. 2017, 27(10): 1249-1267
DOI: 10.1007/s11442-017-1433-1

The mechanism of barrier river reaches in the middle and lower Yangtze River

YOU Xingying[1,2], TANG Jinwu[3], ZHANG Xiaofeng[1], HOU Weiguo[3], *YANG Yunping[4], SUN Zhaohua[1], WENG Zhaohui[2]

1. State Key Laboratory of Water Resource and Hydropower Engineering Science, Wuhan University, Wuhan 430072, China;
2. Hubei Provincial Water Resources and Hydropower Planning Survey and Design Institute, Wuhan 430064, China;
3. Changjiang Institute of Survey Planning Design and Research, Wuhan 430010, China;
4. Key Laboratory of Engineering Sediment, Tianjin Research Institute for Water Transport Engineering, Ministry of Transport, Tianjin 300456, China

Abstract: Alluvial channel has always adjusted itself to the equilibrium state of sediment transport after it was artificially or naturally disturbed. How to maintain the equilibrium state of sediment transport and keep the river regime stable has always been the concerns of fluvial geomorphologists. The channel in the middle and lower reaches of the Yangtze River is characterized by the staggered distribution of the bifurcated river and the single-thread river. The change of river regime is more violently in the bifurcated river than in the single-thread river. Whether the adjustment of the river regime in the bifurcated river can pass through the single-thread river and propagate to the downstream reaches affects the stabilities of the overall river regime. Studies show that the barrier river reach can block the upstream channel adjustment from propagating to the downstream reaches; therefore, it plays a key role in stabilizing the river regime. This study investigates 34 single-thread river reaches in the middle and lower reaches of the Yangtze River. On the basis of the systematic summarization of the fluvial process of the middle and lower reaches of the Yangtze River, the control factors of barrier river reach are summarized and extracted: the planar morphology of single-thread and meandering; with no flow deflecting node distributed in the upper or middle part of the river reach; the hydraulic geometric coefficient is less than 4; the longitudinal gradient is greater than 12‰, the clay content of the concave bank is greater than 9.5%, and the median diameter of the bed sediment is greater than 0.158 mm. From the Navier-Stokes equation, the calculation formula of the bending radius of flow dynamic axis is deduced, and then the roles of these control factors on restricting the migration of the flow dynamic axis and the formation of the barrier river reach are analyzed. The barrier river reach is considered as such when the ratio of the migration force of the flow dynamic axis to the constraint force of the channel boundary is less than 1 under different flow levels. The mechanism of the barrier river reach is

Received: 2016-12-30 **Accepted:** 2017-01-23
Foundation: National Natural Science Foundation of China, No.51379155, No.51339001, No.51579185; National Key Research Program of China, No.2016YFC0402306, No.2016YFC04022310, No.2016YFC0402106; Central Public Research Institutes Fundamental Research, No.TKS160103

Author: You Xingying (1986–), specialized in river bed evolution. E-mail: you_tang@foxmail.com
***Corresponding author:** Yang Yunping (1985–), PhD, E-mail: yangsan520_521@163.com

such that even when the upstream river regime adjusts, the channel boundary of this reach can always constrain the migration amplitude of the flow dynamic axis and centralize the planar position of the main stream line under different upstream river regime conditions, providing a relatively stable incoming flow conditions for the downstream reaches, thereby blocking the upstream river regime adjustment from propagating to the downstream reaches.

Keywords: barrier river reaches; flow dynamic axis; channel boundary; the middle and lower Yangtze River

1 Introduction

The middle and lower Yangtze River (hereafter MLYR), also known as the 'Golden Watercourse', is the chief axis of the 'Yangtze River Economic Belts', whose stable river regime not only facilitates flood control safety and unobstructed navigation, but also affects the utilization of water and soil resources, aiding the sustainable development of economy and society in the both sides of riparian. Thus, the significance of stabilizing the river regime of the MLYR is very important. Usually, the river patterns included anastomosed channel, braided channel, single-thread straight channel, and single-thread meandering channel (Schumm, 1985; Knighton and Nanson, 2001; Nanson *et al*., 2010). However, the river pattern with multiple branches in the Yangtze River differed significantly from the above river patterns, and was hence classified as a bifurcated channel (Wang *et al*., 2000).

Studies show that the Shashi-Datong Reach in the MLYR is alternately distributed by the single-thread river and the bifurcated river, whose lengths are 504.8 km and 486.2 km, accounting for 50.9% and 49.1% of the total length of this reach, respectively. The river regime varies violently because the erosion resistance of the river bank of the bifurcated channel is weak, making the channel wide and shallow. The basic regularities of the evolution of the abnormally-curving-bifurcated river are as follows: "the low shoal at the head of the central island is cut and a new central bar is generated → the new central bar develops and moves downstream → the new central bar merges with the old one and disappears". Reaches that exhibit such evolution regularities are the Luxikou and Luohuzhou reaches (Liu *et al*., 2016). The evolution regularities of the straight or curving bifurcated channel are mainly the alternate translocations between the main branches and the distributaries, such as the Xinyuzhou, Tianxingzhou, and Daijiazhou reaches (Li *et al*., 2012). The single-thread straight channel generally follows the evolution regularity of "with the aggradation or degradation of the staggered point bar, the transition section of the main stream line moves upstream or downstream", but the migration amplitude of the main stream line is not as large as that in the bifurcated channel. Most of the concave banks of the single-thread meandering channels have been protected, reducing their susceptibilities to collapse; thus the evolution regularities of "silting-up at the concave bank and scouring at the convex bank" no longer pertain to all of the meandering channels. Obviously, the river regime of the bifurcated channel changes more acutely than single-thread channel and has a greater effect on flood and navigation management. Accordingly, scholars at the water conservancy and the transport agency have extensively researched the bifurcated channel (Luo, 1989; Li *et al*., 2012; Sun *et al*., 2013; Liu *et al*., 2014; Liu *et al*., 2015; Tang *et al*., 2015).

Due to the characteristics of the alternate distribution of the single-thread and bifurcated river reaches, plenty of measured analyses showed that the channel adjustments of some

bifurcated reaches would continue to propagate downstream (Schuurman *et al*., 2016) through the single-thread reaches, such as the Ma'anshan Reach (Tang *et al*., 2015) and Tianxingzhou Reach (Sun *et al*., 2013), which means that the downstream river evolution is also affected by the adjustment of the upstream river regime. Without a doubt, it makes more difficult to predict the evolution trend of the channel and to design the river regulation works. However, in other bifurcated reaches, the channel adjustments will not continue to propagate downstream through the single-thread reach, such as in the case of Longkou Reach (Li *et al*., 2012), resulting in that the influencing factor of its channel evolution remains relatively unitary, and the layout of river regulation works remains relatively simple. Therefore, it is necessary to study the single-thread river reaches, especially the ones that can block the upstream channel adjustment from propagating downstream.

Based on the systematic summaries and in-depth analyses of the long-flow-path and long-term fluvial process regularities in the MLYR, You (2016) proposed a barrier river reach that can prevent the upstream channel adjustment from propagating downstream, and analyzed the basic characteristics of the barrier river reach. Regrettably, the previous study (You *et al*., 2016) emphasized less on the control factors of the barrier river reach, identifying the barrier river reach with strong empirical bias. At the same time, the mechanism blocking the upstream channel adjustment from propagating downstream was not deep enough; this limited its application in the formation and maintenance of the barrier river reach. Based on this premise, this study further analyzes the control factors in the formation of the barrier river reach by deducing the theoretical formula of the bending radius of the dynamic axis of the flow (the line connecting the point of the maximum vertically averaged flow velocity of each cross-section, which can also be called 'the main stream line'), clarifying the role of each control factor on the formation of barrier river reach and dissecting its mechanism. This could provide an important reference for the river regulation works in the MLYR.

2 Study methods and data sources

2.1 Study methods

The Shashi-Datong Reach of the MLYR was investigated. The river bed is mainly composed of fine sand (Zhang *et al*., 2017). Most of the river banks are typical two-layer structures, some of which have protruding nodes with strong erosion resistance. As shown in Figure 1, at the south bank of the Shashi-Datong Reach, there are three separate diversion branches at Songzikou, Taipingkou, and Ouchikou, whose water flows and sediment loads return to the Yangzte River at the confluence of Chenglingji after being stored in and dispatched from the Dongting Lake. The Dongting Lake also has four main confluence branches; they are the Xiangjiang River, Zijiang River, Yuanjiang River, and Lijiang River. The Hanjiang River converges at the north bank of the Chenglingji-Wuhan Reach, and the Poyang Lake converges at the south bank of Wuhan-Hukou Reach. The Shashi, Jianli, Luoshan, Hankou, Hukou, and Datong hydrological stations are located in sequence along the flow path.

Two main research methods were used in this study. First, the measured hydrological, topographical, geological, and remote sensing data were systematically analyzed to acquire the

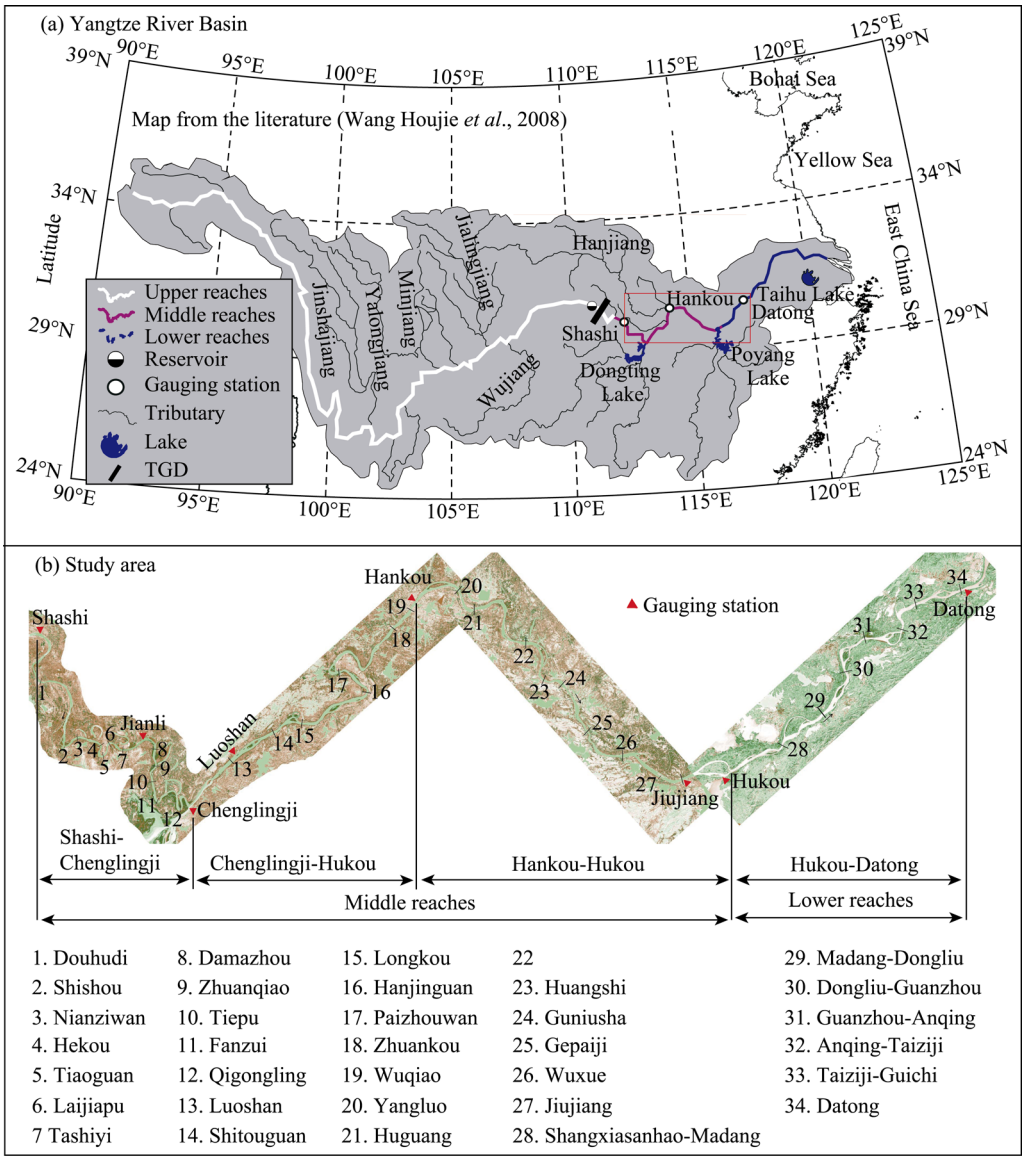

Figure 1 The Yangtze River Basin and the study area

control factors. The detailed method was as follows: using the latest aerial photos, the curvature radius of the river bend was directly measured, and the location and the protruding length of the node could also be measured. The hydraulic geometry of the typical cross-section and the channel longitudinal gradient were calculated using the observed channel topography data of 2011 or 2013. According to the data of riverbed material in 2003–2009, the median diameter of bed sediment of each river reach can be obtained to indicate the erosion resistance factor of riverbed. The geological structure of the concave bank of each river reach from the bankfull water level to the thalweg (the connection line of the lowest point of each topographic cross-section) elevation was systematically summarized, and the clay content of each soil layer was acquired from the test results of physical and mechanical properties. The river bank erosion resistance factor was determined by the weighted average calculating of the thickness of each soil. Through the above methods, the

similarities and differences between the barrier and non-barrier river reach were compared and analyzed from the planar, cross-sectional, longitudinal profile, and riverbed and river bank perspectives; thus the control factors of barrier river reach could be dissected.

Secondly, the formula of the bending radius of flow dynamic axis was derived using the mathematical method, starting from the NS equations, which was half experiential and half theoretical. Then, the contrast relationship between the migration force of the main stream and the constraint force of the channel boundary was stretched out. Consequently, the mechanism of barrier river reach was clarified by verifying the effect of the above control factors on the barrier river reach, combining the observed hydrological, topographical, and geological data.

2.2 Data sources

Aerial photographs from the Landsat satellite digital products of 2016 could be available at the U.S. Geological Survey website (*https://www.usgs.gov/* The Chinese mirror website is: *http://www. gscloud.cn/*). The fielded channel topographical data came from Wuhan University. The data on geological structures and clay contents of the river bank came from the Geological Survey Reports of various embankment sections in the MLYR, and were compiled by the Hubei Provincial Water Resources and Hydropower Planning Survey and Design Institute. The riverbed material data were provided by the Tianjin Research Institute for Water Transport Engineering. The 34 investigated river reaches are distributed in Shashi-Chenglingji Reach, Chenglingji-Wuhan Reach, Wuhan-Hukou Reach, and Hukou-Datong Reach respectively, whose river patterns include both the straight and meandering rivers with single-thread channels, and thus having strong representativeness. Their basic situation and the control factors of barrier are shown in Table 1.

3 Analysis of control factors of barrier properties

3.1 Planar control factors

As can be seen from Table 1, the Tiepu, Luoshan, Zhuankou, Wuqiao, Bahe, and Datong reaches are the single-thread straight reaches. Owing to the wider channels, it is difficult to restrict the changes of the incoming flow directions caused by the adjustments of upstream river regime. Along with the periodically repetitious evolution of the staggered point bar, their flow dynamic axes move upstream or downstream drastically. In contrast, the sinuosities of the Tiaoguan, Tashiyi, and Fanzui reaches are relatively greater; the variation amplitudes of the outflow directions of these river reaches caused by the different incoming flow directions or different flow levels can be limited to a smaller extent, so that these river reaches are effective for restricting the dynamic axes. In the 34 single-thread reaches of Table 1, only the single-thread meandering reaches may have barrier properties, yet the single-thread straight reaches do not have barrier properties, showing that the planar morphology of single-thread meandering is one of the control factors shaping the barrier river reach and blocking the river regime adjustment further downstream.

The nodes in the middle and lower Yangtze River include the rocks protruding from the river bank, cement nozzle, and several years-old aggradational clay layers. The unilateral node distributed in the upper or middle part of the river reach alters the continuities of the planar and transversal morphologies, causing a violent mutation of the bending radius of

Table 1 Barrier control factors of single-thread reaches in the middle and lower Yangtze River

Reach	No.	Reach name (Abbreviation)	Reach length (km)	Distance from Yi-chang (km)	River pattern	Presence location of flow deflecting nodes	Hydraulic geometric coefficient	Presence of barrier property
Jingjiang	1	Douhudi (DHD)	9.9	175	Single meandering	Non	2.55	Yes
	2	Shishou (SS)	8	234	Single meandering	In the middle	2.86	No
	3	Nianziwan (NZW)	15	242	Single meandering	Non	4.76	No
	4	Hekou (HK)	7	257	Single meandering	Non	3.19	No
	5	Tiaoguan (TG)	13	264	Single meandering	Non	2.61	Yes
	6	Laijiapu (LJP)	12	277	Single meandering	Non	3.32	No
	7	Tashiyi (TSY)	14	289	Single meandering	Non	2.98	Yes
	8	Damazhou (DMZ)	10.5	330	Single meandering	In entrance	6.68	No
	9	Zhuanqiao (ZQ)	9	338	Single meandering	Non	3.66	Yes
	10	Tiepu (TP)	12	347	Single straight	Non	4.31	No
	11	Fanzui (FZ)	6.5	356	Single straight	Non	3.11	Yes
	12	Qigongling (QGL)	7.8	380	Single meandering	In the middle	3.29	No
Chengling-ji-Wuhan	13	Luoshan (LS)	11	419	Single straight	In entrance	6.25	No
	14	Shitouguan (STG)	9	456	Single meandering	In export	5.08	No
	15	Longkou (LK)	9.6	483	Single meandering	In export	3.42	Yes
	16	Hanjinguan (HJG)	10.9	519	Single meandering	Non	3.25	Yes
	17	Paizhouwan (PZW)	15	542	Single meandering	Non	2.14	No
	18	Zhuankou(ZK)	12	610	Single straight	In the middle	5.79	No
	19	Wuqiao (WQ)	13	628	Single straight	In entrance	4.47	No
Wuhan Hukou	20	Yangluo (YL)	15	658	Single meandering	In entrance	3.46	No
	21	Huguang (HG)	10	679	Single meandering	In entrance	3.93	No
	22	Bahe (BH)	9.4	723	Single straight	In entrance	4.52	No
	23	Huangshi (HS)	15.5	753	Single meandering	In export	2.70	Yes
	24	Guniusha (GNS)	17	773	Single meandering	In entrance	4.07	No
	25	Gepaiji (GPJ)	15	802	Single meandering	Along both banks	0.79	Yes
	26	Wuxue (WX)	13	830	Single meandering	In entrance	4.87	No
	27	Jiujiang (JJ)	16	853	Single meandering	Non	3.17	No
Hukou-Datong	28	Shangxiasanhao-Madang (SXSH-MD)	6	938	Single meandering	In export	2.05	Yes
	29	Madang-Dongliu (MD-DL)	8	972	Single meandering	Non	2.96	Yes
	30	Dongliu-Guanzhou (DL-GZ)	9	995	Single meandering	In the middle	3.47	No
	31	Guanzhou-Anqing (GZ-AQ)	16	1023	Single meandering	In the middle	2.71	No
	32	Anqing-Taiziji (AQ-TZJ)	8.4	1054	Single meandering	In export	1.71	Yes
	33	Taiziji-Guichi (TZJ-GC)	10.5	1078	Single meandering	Non	4.16	No
	34	Datong (DT)	16	1101	Single straight	In entrance	4.29	No

the flow dynamic axis. After the upstream channel adjustment, the angle of the incoming flow exerting on the node will change, and the proximity degree of the flow dynamic axis to

the node will also change (Liu *et al*., 2015), altering the intensity of the node deflecting flow, resulting in a great variation of the direction of the dynamic axis of outflow.

There are also a large number of bilateral nodes distributed in the middle and lower Yangtze River. As a river channel boundary has greatly resistance to the erosion of water flow, the bilateral nodes are favorable for limiting the channel widening and controlling the integral morphology of the channel (Luo *et al*., 1987; Qian *et al*., 1989). However, due to that the different nodes have different deflecting flow strengths, if the upstream river regime changes, there will be a strength difference when the bilateral nodes deflect flow alternately. The geological compositions of the both banks in downstream river are also different, thus the main stream line will migrate and the river regime will be altered. For example, the YangLin Node and the Longtou Mountain are distributed bilaterally at the entrance of the Luoshan Reach. Due to the different strengths of deflecting flow of the two nodes (Leng, 1993), the downstream main stream lines migrate frequently, and taking into account the weak erosion resistance of the river bank of the downstream Jiepai Reach, both the broadening of the channel and the amplifying of the migration amplitude of the main stream line may occur (Liu *et al*., 2014). This kind of river reach does not have barrier properties. The Wuqiao Reach with the Turtle and Snake Mountains at its entrance also has similar characteristics.

Some river reaches with bilateral nodes at the entrance are relatively stable, such as the Bailuo and Daoren Nodes distributed in the Nanyang Reach, and the Shamao and Tieban Nodes distributed in the Tieban Reach. The stabilities of their river regimes are dependent on the long-term stabilization of their upstream river regimes, such as in the case of the Guanyin and Meitan reaches, which respectively provides stable planar locations for the incoming flow of the downstream Nanyang and Tieban reaches, resulting in only minor changes in the deflecting flow strengths of the nodes. Therefore, the stabilization of their river regimes depends on the stabilization of their upstream river regimes. Once the upstream river regime is adjusted by the artificial and natural disturbances, the river regime of this reach will be adjusted accordingly. However, it is difficult to maintain the narrow and deep cross-section to restrict the migration of the main stream line after the river regime adjustment at the entrance which is caused by the difference in the deflecting flow strengths of the bilateral nodes (Leng, 1993) or the difference of the geological and geomorphological conditions of both bank sides of downstream (Yu, 1984). Thus, the river reaches with bilateral nodes usually do not have barrier properties.

3.2 Cross-sectional control factors

It is difficult to prevent the flow dynamic axis from migrating in the wider channels, and floodplains are generally known to occur in their vicinity (Ramos and Gracia, 2012; Clerici *et al*., 2015). When water overflows from the deep channel and enters the floodplain, the channel width increases abruptly, and the hydraulic geometric coefficient ζ (where $\zeta=\sqrt{B}/h$, B is river width, h is river depth) also increases significantly (Regalla *et al*., 2013), providing sufficient migrating space for the flow dynamic axis. At this time, the upper river regime adjustment is bound to cause the migration of the flow dynamic axis and propagate downstream.

Figure 2 depicts the typical cross-sections of each river reach, in order to be more obvious, the thalweg of the narrow and deep cross-sections are drawn on the left side of the dividing

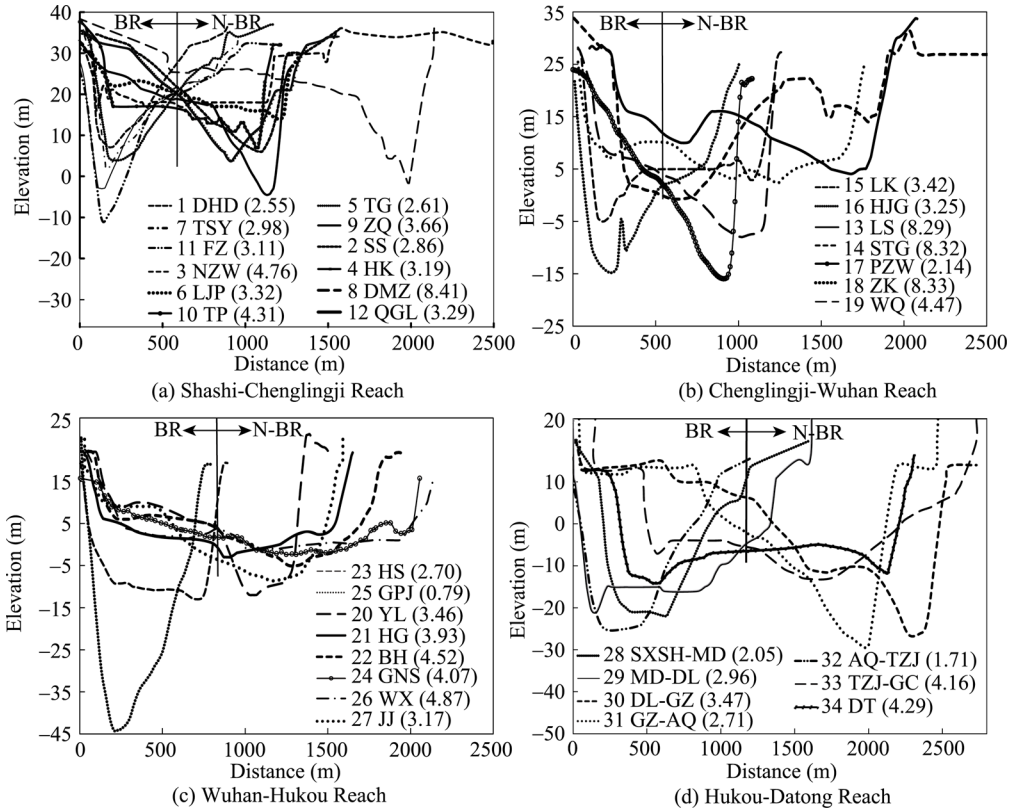

Figure 2 The configurations of the typical cross-section of the single-thread reaches in the middle and lower Yangtze River

Note: BR means barrier river reaches, and N-BR means non-barrier river reaches in the above figure.

line in this figure, and other cross-sections are drawn on the right side of the dividing line. It is seen that on the left side of the dividing line, the river reaches with narrow and deep cross-sections, including the Douhudi, Tiaoguan, Tashiyi, Zhuanqiao, Fanzui, Longkou, Hanjinguan, Huangshi, Gepaiji, Shangxiasanhao-Madang, Madang-Dongliu, and Anqing-Taiziji reaches, all of which have barrier properties. Their average hydraulic geometric coefficients ζ under different flow levels are all smaller than 4. With the increase of the flow level, the river width increases less but the water depth increases more, thus maintaining the flow dynamic axis stable and preventing the upstream channel adjustment from transferring downstream. Besides the straight reaches and the reaches with nodes, the Nianziwan, Damazhou, Shitouguan, and Taiziji-Guichi reaches, whose average hydraulic geometric coefficients under different flow levels are greater than 4, have no barrier properties. Thus, $\zeta<4$ is also one of the control factors in the formation of barrier river reaches and in the blocking process of the upstream channel adjustments propagating downstream.

3.3 Longitudinal profile control factors

For the river reaches with the positive slopes, whose thalweg elevation at the entrance is higher than at the export, the steeper the river longitudinal profile, the greater the channel longitudinal gradient. The strong suction effect at the export of river reach concentrates the

flows from different upstream directions and prevents the flow dynamic axis from migrating. There are two kinds of manifestations: One is the scour holes at the export of the river reach caused by the nodes deflecting flow, such as in the Longkou, Huangshi, and Gepaiji reaches. The other is the scour holes formed by the circulation effect of the concave bank of the river bend, such as in the Tiaoguan, Fanzui and Hanjinguan reaches. The river reaches with negative slopes, or the reaches having backwater effects caused by tributaries confluences at the exports, usually do not possess barrier properties. Statistics show that (Figure 3), except for the reaches with straight morphologies, or the flow deflecting nodes, or $\zeta > 4$, in the remaining 17 single-thread reaches, only the Qigongling, Paizhouwan, and Jiujiang reaches have no barrier properties because their channel longitudinal gradients are less than 12‰, while all the other 14 reaches have gradients greater than 12‰. This shows that the channel longitudinal gradient greater than 12‰ is also one of the influencing factors in the formation of barrier river reach and in the blocking process of the upstream river regime adjustments propagating downstream.

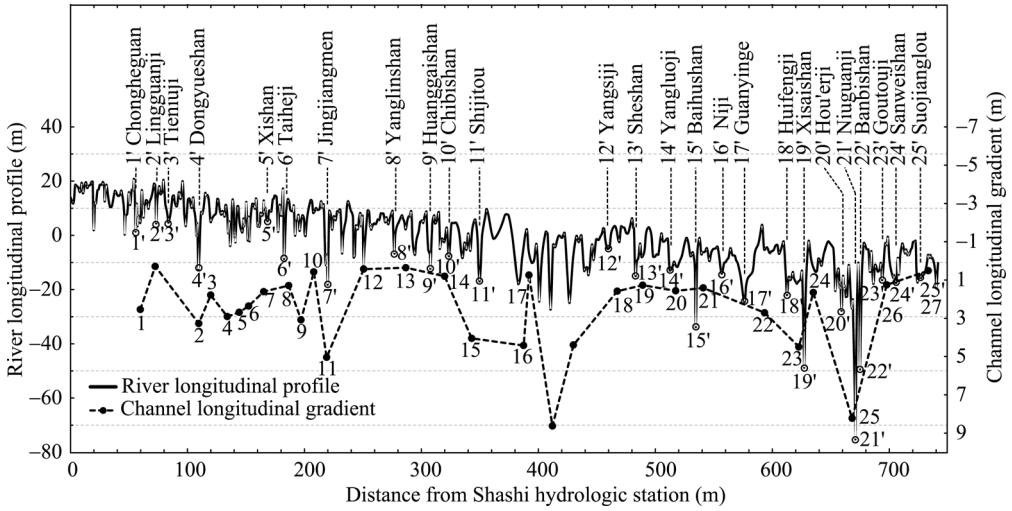

Figure 3 The channel longitudinal gradients of the single-thread reaches and the longitudinal profile of the middle and lower Yangtze River

3.4 Riverbank and riverbed control factors

Julian and Torres (2006) considered the erosion resistance to be proportional to the silty clay content. Figure 4 shows the clay contents of the concave banks and the median diameters of the bed materials. Out of the remaining 14 river reaches, only the clay contents of the concave banks of the Hekou and Laijiapu reaches are lower than 9.5%, having no barrier properties, while the other 12 river reaches are higher than 9.5%. Only the median diameter of the bed material of the Hekou Reach is finer than 0.158 mm, having no barrier property, while the other 12 river reaches are coarser than 0.158 mm. It is thus clear that only the river bank having stronger erosion resistance can block the collapse or the broadening of the channel. The river reach itself can maintain a stable river regime and make the meandering morphology and the narrow and deep cross-section unchanged, so as to restrict the migration of flow dynamic axis. Only when the riverbed sediment is coarser, the erosion resistance is

stronger, and the moving bed resistance is larger; the configuration of the point bar and pool in this reach will be difficult to change (Wohl, 2015), and it will be difficult for the flow dynamic axis to migrate drastically. Thus the control factors on the formation of the barrier river reach also include that the clay content of concave bank is higher than 9.5%, and the median diameter of bed sediment is coarser than 0.158 mm. It is worth noting that the accumulated bank protection volume is, on average, 189.1 m^3/m in barrier reaches, but only 126.9 m^3/m in non-barrier reaches, illustrating that the natural geological conditions of the river banks in some barrier reaches have relatively weaker erosion resistances, such as in the case of the Tiaoguan, Tashiyi, Zhuanqiao, and Fanzui reaches. To counteract the weaker erosion resistances of their river banks, their volumes of bank protection are greater, so as to ensure the overall stronger resistances to the erosion of water flow.

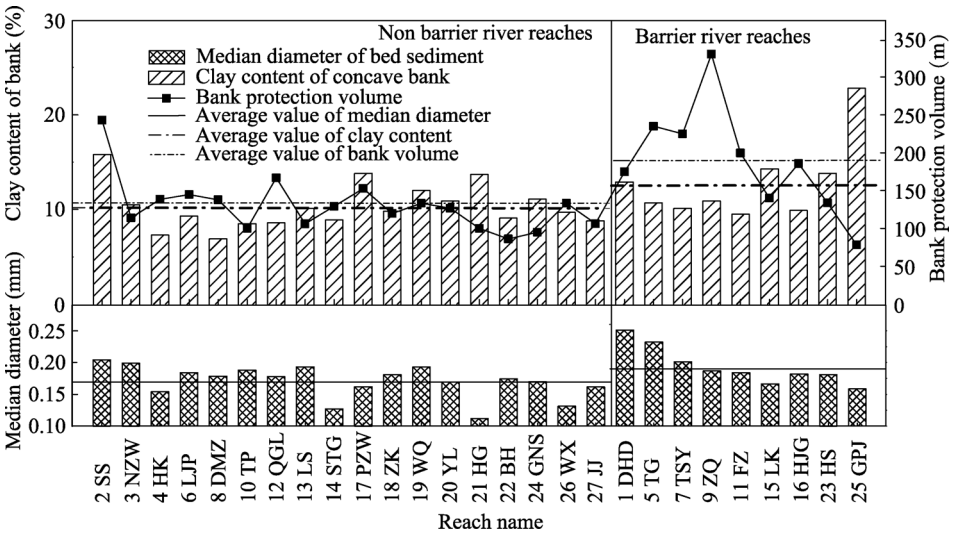

Figure 4 The river bank clay content and the median diameter of bed sediment of the single-thread reaches in the middle and lower Yangtze River

4 Analysis of mechanism of river reach barriers

Studies (You *et al*., 2016) showed that the essence of the downstream propagating of the river regime adjustment is the downstream propagating of the change of planar position of the main stream line. The above analysis showed that only the single-thread river bend could have barrier properties, and the bending radius of the flow dynamic axis can reflect the planar position of the main stream line of the natural river bend very well. Thus, the migration of the main stream line is reflected by the change of the bending radius of the flow dynamic line. Based on this, in this section, the bending radius of the flow dynamic axis is deduced, the effects of the above control factors on the barrier properties are analyzed, and the mechanism of the barrier river reach is also clarified.

4.1 The theoretical solution for the bending radius of the flow dynamic axis

4.1.1 Formula derivation

The expression for the three-dimensional flow dynamic equations such as the Navier-Stokes equation (Domenichini and Baccani, 2004) is as follows:

$$\frac{\partial u_i}{\partial t}+u_j\frac{\partial u_i}{\partial x_j}=-\frac{1}{\rho}\frac{\partial p}{\partial x_j}+\frac{1}{\rho}\frac{\partial}{\partial x_j}\left(\mu\frac{\partial u_i}{\partial x_j}\right)-\frac{\partial}{\partial x_j}\left(\overline{u_i'u_j'}\right) \tag{1}$$

Neglecting the turbulent diffusion term and non-constant term, and the bottom resistance term commonly using the item of $\frac{gn^2}{h^{1/3}}u\sqrt{u^2+v^2}$, the two-dimensional steady flow dynamic equation under the polar coordinate can be deduced as follows:

$$\frac{u}{R}\frac{\partial u}{\partial \varphi}+v\frac{\partial u}{\partial R}+\frac{uv}{R}=-\frac{1}{\rho R}\frac{\partial p}{\partial \varphi}+gJ_\varphi-\frac{gn^2}{h^{4/3}}u\sqrt{u^2+v^2} \tag{2}$$

where φ and R are the sinuosity of the bend (in radians) and the bending radius at the perpendicular line, respectively. u and v are the average velocity of the perpendicular line at (φ_0, R_0), respectively. J_φ is the water surface longitudinal gradient, h is the water depth at the perpendicular line, p is the hydrodynamic pressure, g is the acceleration due to gravity, and ρ is the density of water. Then, the Manning Formula and the Chezy Coefficient are taken into the bottom resistance term:

$$\frac{gn^2}{h^{4/3}}u\sqrt{u^2+v^2}=\frac{gu^2}{hC^2} \tag{3}$$

Considering that the transverse flow velocity is much smaller than the longitudinal flow velocity, the terms with v are ignored. Given that the hydrodynamic pressure is generated by the wall shear stress, p can be expressed as the integral form of the wall shear stress τ (N^2/m) along the perpendicular line, $p=-\int_{z=0}^{z=\varsigma}\tau dz=-\tau h$, then Eq. 3 can be transformed into:

$$\frac{1}{2Rg}\frac{\partial u^2}{\partial \varphi}=\frac{1}{\rho gR}\frac{\partial(\tau h)}{\partial \varphi}+J_\varphi-\frac{u^2}{hC^2} \tag{4}$$

Yin (1965) summarized a better relationship between the riverbed roughness and the downstream limit particle size of the coarsening layer as $n=d^{1/6}/21=0.048d^{1/6}$, according to the measured data and flume test data. Xu (1997) believed that the relationship between the critical scour shear stress of the riverbed τ_c and the clay content of the bed material M_0 was basically proportional, $\tau_c=0.254M_0^{0.99}$, according to the 16 groups of test data of Dunn (1959). But Lane (1959) discovered that the shear stress near the river banks is close to 0.76 times the shear stress near the riverbed, so the wall shear stress is expressed as $\tau=0.193M^{0.99}$, where M is the clay content of the bank.

Taking the Chezy coefficient $C=h^{1/6}/n$ into account, $C=21(h/d)^{1/6}$. Eq. 5 shows the substitution of the above results into Eq. 4：

$$\frac{1}{2Rg}\frac{\partial u^2}{\partial \varphi}=\frac{1}{\rho gR}\frac{\partial\left(0.193M^{0.99}h\right)}{\partial \varphi}+J_\varphi-\frac{u^2d^{1/3}}{441h^{5/3}} \tag{5}$$

Then, u^2 is solved using a first order ordinary differential equation, assuming that all the

hydraulic factors in the curve do not change significantly within a certain flow pathway. The flow velocity average along the perpendicular line at the entrance of the river bend is approximated as $u = Q/(Rh \cdot \ln(R_2/R_1))$ (Zhang, 1984). Considering that the river width (B) is smaller than the curvature radius of the curve (R_*) in most cases, $\ln\frac{R_2}{R_1} = \frac{B}{R_*}$, $u = \left.\frac{R_* Q}{RBh}\right|_{\varphi=0}$, and u can be expressed as:

$$u = \sqrt{N \cdot S + \left[\left(\frac{R_* Q}{RBh}\right)^2 - N \cdot S\right] e^{-\frac{2gR\varphi d^{1/3}}{441h^{4/3}}}} \tag{6}$$

where $N = J + \frac{0.193M^{0.99}h}{gR\rho}$, $S = \frac{441h^{4/3}}{d^{1/3}}$. Given that the water flow velocity, the water depth, and the water surface longitudinal gradient, all achieve their maxima at the flow dynamic axis, $\left.\frac{\partial u}{\partial R}\right|_{R=R_0} = 0$, $\left.\frac{\partial J}{\partial R}\right|_{R=R_0} = 0$, $\left.\frac{\partial h}{\partial R}\right|_{R=R_0} = 0$. The hydraulic geometric coefficient is introduced by $\varsigma = \sqrt{B}/h$, accordingly, $B \cdot h = \varsigma^2 h^3$.

Taking the derivative of R in Eq. 6, the mathematical expression directly describing the variation in the bending radius of the flow dynamic axis can be derived:

$$\left(\frac{R_* Q}{\varsigma^2 h_0^3}\right)^2 \frac{1}{R_0^3} + \left(\frac{R_* Q}{\varsigma^2 h_0^3}\right)^2 \frac{1}{R_0^2} \frac{g\varphi d^{1/3}}{441h_0^{4/3}} - \frac{M' g\varphi d^{1/3}}{\rho h_0^{1/3}} - gJ_0\varphi = 0 \tag{7}$$

where $M' = 0.0009M^{0.99}$. The theoretical equation of R_0 at the flow dynamic axis line can be solved by Eq. 7:

$$R_0 = \left[\frac{R_*^2 Q^2 \rho}{\varphi g \varsigma^4 h_0^5 (\rho J h_0^{2/3} + M' d^{1/3})}\right]^{1/3} \tag{8}$$

The middle and lower Yangtze River, where the Dongting Lake, Poyang Lake, Hanjiang River and other tributaries converge into the trunk stream of the Yangtze River along the flow pathway, is largely alluvial; thus the annual and interannual variation amplitude of flow is very large (Xia *et al*., 2016; Mossa, 2016). Therefore, $\frac{Q_{\max} - Q_{\min}}{Q_{\max}}$ is added to represent the role of the variation amplitude of the flow rate on the flow dynamic axis.

Secondly, the larger the relative length of the node protruding from the river bank line, the greater the constriction degree of the river width, the stronger the deflecting flow capacity of the node, and the larger the migration magnitude of the flow dynamic axis. Thus $\lambda = \frac{B_{bankfull} - L_{node}}{B_{bankfull}}$ is taken to indicate the influence of the deflecting flow strength of the node. For the same node, the strength of deflecting flow changes when the flow level changes. Under different flow levels, the proximity degree of the flow dynamic axis to the node is usually different; thus the deflecting strength of the node is different too. The smaller the value of λ, the more sensitive the node's response to the change of incoming flow level,

so $1/\lambda$ is taken as the coefficient of the variation amplitude of the flow.

$$R_0 = \left[\frac{R_*^2 \left(\frac{Q}{\lambda} \cdot \frac{Q_{\max} - Q_{\min}}{Q_{\max}} \right)^2 \rho}{\varphi g \varsigma^{4\lambda} h_0^5 \left(\rho J h_0^{2/3} + M' d^{1/3} \right)} \right]^{1/3} \tag{9}$$

where $Q_{\max}$ and $Q_{\min}$ are the maximal and minimal flow rates of the river reach, respectively; $B_{bankfull}$ is the bankfull river width, and L_{node} is the protruding length of the node from the river bank line. It should be noted that although Eq. 9 is deduced from the NS equation, the empirical formulas are also used in the derivation procedure, making Eq. 9 a semi-empirical semi-theoretical formula.

4.1.2 Analysis of the formula rationality

Numerous scholars (Zhang *et al.*,1983; Zhang *et al.*,1984; Qian, 1987) have done extensive researches on the formulas of the bending radius of the flow dynamic axis in the river bend, and put forward many semi-empirical semi-theoretical or empirical formulas. All of them considered that the bending radius of the flow dynamic axis was positively correlated with the flow rate, which was consistent with the general regularity of "the flow dynamic axis went straight during floods, but bent during the dry season". It can be seen that the bending radius of the flow dynamic axis derived in Eq. 9 was also positively correlated with the flow rate, which was in accordance with the existing researches.

At the same time, the existing research (Yu *et al.*, 1987; Luo *et al.*, 1989; Leng *et al.*, 1993; Li *et al.*, 2012; Liu *et al.*, 2015; You *et al.*, 2016) gradually recognized the important role of the flow deflecting node on the fluvial process. Based on this, Eq. 9 considers the effect of the node, which is the main difference comparing with the existing research results. In order to verify the rationality of Eq. 9, taking the Guniusha Reach as an example, the bending radii of the flow dynamic axis at several typical cross-sections under different flow levels are calculated using both Eq. 9 and the existing other formulas. The comparisons of their results with the measured values are shown in Table 2 and Figure 5. It can be seen that the results from Eq. 9 are more consistent with the measured values, indicating that Eq. 9 is more suitable for the calculation of the bending radius of the flow dynamic axis when there is flow deflecting node distributed at the entrance of the river reach, as in the case of the Guniusha Reach.

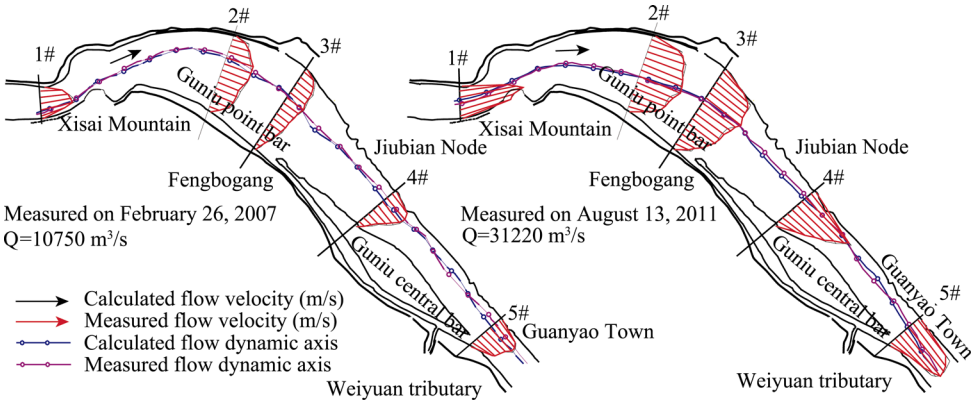

Figure 5 The verification of the flow dynamic axis calculated by Eq.9 in the Guniusha Reach

Table 2 The comparison of the formula results with the measured values in the Guniusha Reach

Measured values	Q (m^3/s) / Bending radii of flow dynamic axis /m / Formulas	2# Q=10750 m^3/s	3# Q=31220 m^3/s	2# Q=10750 m^3/s	3# Q=31220 m^3/s	2# Q=10750 m^3/s	3# Q=31220 m^3/s
		2530	2900	2820	3940	3090	3750
Eq. 9	$R_0=\left[\frac{R_*^2\left(\frac{Q}{\lambda}\cdot\frac{Q_{\max}-Q_{\min}}{Q_{\max}}\right)^2\rho}{\varphi g\varsigma^{4\lambda}h_0^5\left(\rho Jh_0^{2/3}+M'd^{1/3}\right)}\right]^{1/3}$	2498	2976	2782	3997	3133	3771
Lvtai Ouyang (1987)	$R=48.1\left(QJ^{1/2}\right)^{0.83}$	2390	3771	2390	3771	2390	3771
Zhang (1983)	$R=0.26R_*^{0.73}\left(\sqrt{B}/h\right)^{0.73}\left(Qh^{2/3}J^{1/2}\right)^{0.23}$	851	890	1549	1919	1814	2246
Zhang (1984)	$R_0=\sqrt[3]{\frac{1}{\varphi Jg}\left(\frac{R_*Q}{A}\right)^2}$	2204	3597	2056	3531	2163	3446

4.2 Analysis of mechanism of river reach barriers

4.2.1 Mechanisms of various control factors barriers

Eq. 9 could be transformed as:

$$\frac{R_0}{R_*}=\frac{\left[\left(\frac{Q}{\sqrt{R_*}}\cdot\frac{Q_{\max}-Q_{\min}}{\lambda Q_{\max}}\right)^2\frac{\varsigma^{(5-4\lambda)}}{\varphi}\right]^{1/3}}{\left[gB^{5/2}\left(Jh_0^{2/3}+\frac{M'd^{1/3}}{\rho}\right)\right]^{1/3}}\approx\frac{F_{migration}}{F_{constraint}}=\frac{F_m}{F_c} \tag{10}$$

where the term of R_0/R_* on the left side can be used to indicate the constraint effect of curvature radius of the river bend on the bending radius of the flow dynamic axis. Obviously, the smaller this value, the greater the constraint effect of the curvature radius of the river bend on the bending radius of the flow dynamic axis. Then the smaller the migration amplitude of the main stream line, the more likely for the river reach to have barrier properties.

If the flow process is constant, the planar position of the flow dynamic axis will not change with the temporal and spatial variation, and there will be no adjustment for the river regime. Thus, the change of the flow process is a dynamic factor which promotes the migration of the flow dynamic axis. Analyses of Chapter 3 of Qian's work (1987) show that the flow deflecting nodes distributed in the upper or middle parts of the river reaches exacerbates the migration amplitudes of the flow dynamic axes under different flow levels. For the straight river reach with an undersized sinuosity, in which the difference between the curvature radius of the river bend and the bending radius of the flow dynamic axis is large, the concentrating action of the river reach on the flow dynamic axis will be weakened (Qian, 1987). The wide and shallow cross-section with an oversized hydraulic geometric coefficient often provides a larger migration room for the flow dynamic axis, while the smaller altitudinal difference between point bar and pool will also be beneficial for the chute cutoff. Thus, the variability of the flow process, the existence of the flow deflecting node, the small sinuosity of the river bend, and the large hydraulic geometric coefficient all promote the migra-

tion of the flow dynamic axis. The numerator on the right side of Eq. 10 can be taken as the migration force of the flow dynamic axis.

Analyses of Chapter 3 show that, when the channel longitudinal gradient magnifies, the stream power per unit width will increase, leading to the erosion and deposition of the deep channel, thereby facilitating the restriction of the lateral shift of the flow dynamic axis. The river bank with the higher clay content has stronger resistance to the erosion of water flow, and thus is beneficial in shaping the cross-section with narrow and deep configuration and in reducing the lateral moving space of the flow dynamic axis. When the riverbed sediment is coarser, the riverbed has greater resistance to the erosion of the water flow, and to a certain extent, resulting in the reduction of the migration amplitude of the flow dynamic axis. Therefore, a large channel longitudinal gradient, with the strong erosion resistances of the river bank and the riverbed can restrict the migration of the flow dynamic axis. The denominator item on the right side in Eq. 10 can be seen as the constraint force of the channel boundary.

In the above analysis, the right side of Eq. 10 approximately reflects the contrasting relationship between the migration force of the flow dynamic axis and the constraint force of the channel boundary, and macroscopically, manifests the contrasting relationship between the bending radius of the flow dynamic axis and the curvature radius of the river bend. It is thus evident that the above formula structure is reasonable. The function of the control factors on promoting or restricting the migration of the flow dynamic axis that is analyzed in Chapter 3 is reasonable too.

In order to further analyze the influence degrees of different control factors on the migration of the flow dynamic axis, sorting out the variation ranges of each control factor is done as follows: the flow level is in the range of 4000–80,000 m³/s, the curvature radius of the river bend is 2000–16000 m, the hydraulic geometric coefficient is 0.8–6.7, the relative length of the node protruding from the river bank line is 0.67–1.0, the channel longitudinal gradient is 4‰–82‰, the median diameter of bed material is 0.112–0.251 mm, and the clay content of the concave bank is 6.9%–22.8%. Therefore, making any control factor in the above-mentioned range relatively changed and other control factors in their own average value unchanged, the sensitivity of the Ψ to the relatively change of the each control factor can be analyzed and shown in Figure 6.

As shown in Figure 6, F_m/F_c is directly proportional to Q and R^*, but inversely proportional to ζ, λ, M, J and d. The absolute values of the gradients of the correlation curves show a variation regularity of $Q > \varsigma > R_* > \lambda > M > J > d$. Firstly, the change of Q is bound to cause the migration of the flow dynamic axis, and only the cross-section with deep and narrow configuration can have greater constraint force to restrict the migration of the main stream line. This is an essential element in the formation of the barrier river reach. Secondly, the planar morphology of single-thread and meandering without the flow deflecting node in the upper and middle part of the river reach can form the cross-section which is reciprocally adaptive to the water flow, thereby restricting the migration of the main stream line. Only the river reach whose river bank has greater erosion resistance can maintain the long-term narrow and deep cross-section. Again, the steep channel longitudinal gradient and the coarse riverbed median diameter are propitious in concentrating the water flow into deep channels and letting them down, thereby reducing the lateral shift of the main stream line. Therefore,

the six control factors above-mentioned in the final analysis together shape a narrow and deep cross-section to constrain the migration of the main stream line. They are all essential.

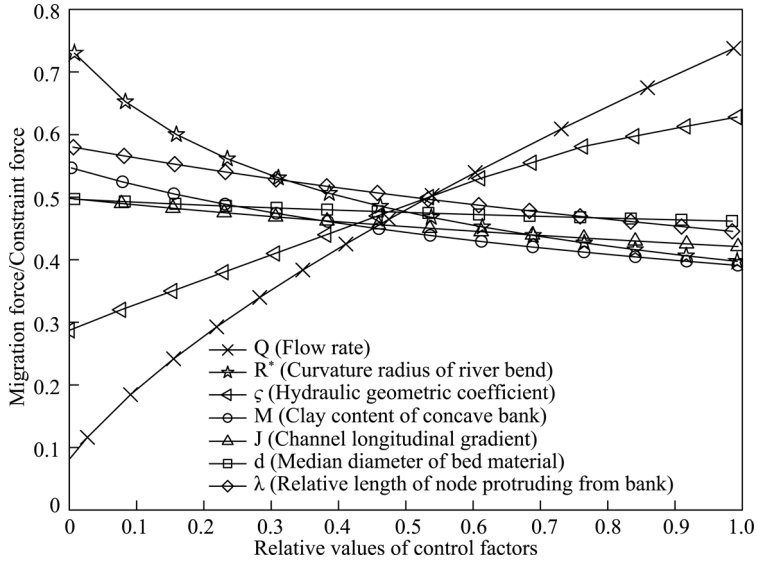

Figure 6 Sensitivity analysis of the influences of various control factors on the barrier river reaches

4.2.2 The ratio of the migration force of the flow dynamic axis to the constraint force of the channel boundary determines the barrier properties of the river reach

According to Eq. 10, the values of F_m/F_c of the 34 river reaches were calculated, and their variation trends with the changes of Q values were shown in Table 1. As shown in Figure 7, the ratios of the migration forces of the main stream to the constraint forces of the channel boundary magnifies with the increase of Q values. Combining with Table 1, it can be seen that, the ratios of the migration force to the constraint force are always less than 1 in the Douhudi, Tiaoguan, Tashiyi, Zhuanqiao, Fanzui, Longkou, Hanjinguan, Huangshi, Gepaiji, Shangxiasanhao-Madang, Madang-Dongliu, and Anqing-Taiziji reaches, which have barrier properties. It is illustrated that under different flow levels, their constraint forces of the channel boundaries are larger than the migration forces of the main streams; thereby effectively restricting the migration of the main stream line, resulting in the development of barrier properties. However, the non-barrier river reaches whose constraint forces of the channel boundaries are smaller than their migration forces of the main streams when the flow rates exceed certain values, cannot restrict the migrations of the main streams effectively, resulting in the destruction of barrier properties.

In conclusion, the mechanism of the barrier river reach is dependent on the constraint force of its channel boundary being always greater than the migration forces of the main stream under different flow levels. Even if the upstream river regime changes obviously and the direction of the incoming flow changes drastically, the channel boundary of this river reach can always restrict the planar position of the flow dynamic axis and weaken the large-scale migration of the flow dynamic axis after the upstream river regime adjusts, helping to centralize the planar positions of the flow dynamic axes, and thereby providing relatively stable incoming flow conditions for the downstream reaches.

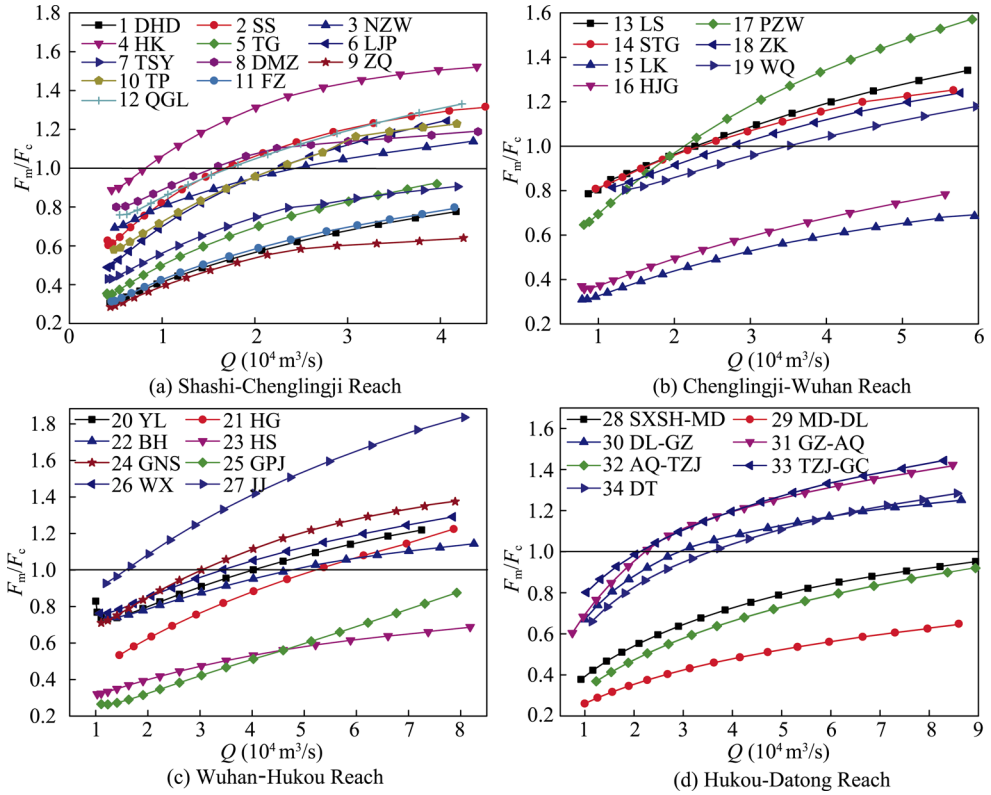

Figure 7 The ratio of the migration force of the flow dynamic axis to the constraint force of the channel boundary in the middle and lower Yangtze River

Chapter 3 analyzes the control factors like planar, transversal, and longitudinal morphologies, and the erosion resistances of the river bank and riverbed, which are the necessary conditions for the constraint force of the channel boundary to be greater than the migration forces of the main stream. For the river reaches that do not meet one or more above conditions, with the changes of the incoming flow direction and the flow level, the constraint force of the channel boundary cannot always be greater than the migration forces of the main stream, resulting in that the planar position of the main stream line changes greatly, and the downstream river regime adjusting accordingly, thus not having the barrier properties.

5 Conclusions

The 34 single-thread river reaches were investigated on the basis of judging whether they have barrier properties or not, and the control factors of the barrier properties were contrasted and analyzed, the calculation formula of the bending radius of the flow dynamic axis was deduced, and the action mechanism of each control factor on the barrier properties was analyzed. The main conclusions are as follows:

(1) The control factors of the barrier river reach include: planar morphology of single-thread and meandering, and without flow deflecting node distributed in the upper or middle part of the river reach. The hydraulic geometric coefficient is less than 4, the channel longitudinal gradient is greater than 1.2‰, the clay content of the concave bank is greater than 9.5%, and the median diameter of the bed sediment is greater than 0.158 mm.

(2) The mechanism of the barrier river reach when the constraint force of the channel boundary is always greater than the migration forces of the main stream under different flow levels. Even if the upstream river regime changes obviously, the channel boundary of this river reach can always restrict the planar position of the flow dynamic axis, and help to centralize the planar positions of the main stream lines under different conditions of upstream river regime, thereby providing relatively stable incoming flow conditions for the downstream reaches.

References

Bandyopadhyay S, Ghosh K, De S K, 2014. A proposed method of bank erosion vulnerability zonation and its application on the River Haora, Tripura, India. *Geomorphology*, 224: 111–121. doi: 10.1016/j.geomorph.2014.07.018.

Bawa N, Jain V, Shekhar S *et al*., 2014. Controls on morphological variability and role of stream power distribution pattern, Yamuna River, western India. *Geomorphology*, 227: 60–72. doi: 10.1016/j.geomorph.2014.05.016.

Clerici A, Perego S, Chelli A *et al*., 2015. Morphological changes of the floodplain reach of the Taro River (Northern Italy) in the last two centuries. *Journal of Hydrology*, 527: 1106–1122. doi: 10.1016/j.jhydrol.2015.05.063.

Domenichini F, Baccani B, 2004. A formulation of Navier–Stokes problem in cylindrical coordinates applied to the 3D entry jet in a duct. *Journal of Computational Physics*, 200(1): 177–191. doi: 10.1016/j.jcp.2004.04.002.

Jason P Julian, Raymond Torres, 2006. Hydraulic erosion of cohesive river banks. *Geomorphology*, 76(1/2): 193–206. doi: 10.1016/j.geomorph.2005.11.003.

Julian J P, Torres R, 2006. Hydraulic erosion of cohesive riverbanks. *Geomorphology*, 76(1/2): 193–206.

Knighton A D, Nanson G C, 2001. An event-based approach to the hydrology of arid zone rivers in the Channel Country of Australia. *Journal of Hydrology*, 254(1): 102–123. doi: 10.1016/S0022-1694(01)00498-X.

Lane E W, 1955. Design of Stable Channels. *Transactions of the American Society of Civil Engineers*, 120(1): 1234–1260.

Langendoen E J, Mendoza A, Abad J D *et al*., 2016. Improved numerical modeling of morphodynamics of rivers with steep banks. *Advances in Water Resources*, 93: 4–14. doi: 10.1016/j.advwatres.2015.04.002.

Leng Kui, 1993. The evolution analysis of Chenluo Reach at the Middle Yangtze River. *Journal of Sediment Research*, (3): 109–116. (in Chinese)

Li Yitian, Tang Jinwu, Zhu Lingling *et al*., 2012. Evolution and Waterway Regulation of the Middle and Lower Yangtze River. Beijing: China Water Conservancy and Hydropower Press, 78–89. (in Chinese)

Liu Lin, Huang Chengtao, Li Ming *et al*., 2014. Periodic evolution mechanism of staggered beach in typical straight reach of the middle Yangtze River. *Journal of Basic Science and Engineering*, 22(3): 445–456. (in Chinese)

Liu Ya, Wang Fei, Li Yitian, 2015. Objective river pattern of waterway regulation of goose-head-shaped anabranching channel in the Middle and Lower Yangtze River. *Journal of Hydraulic Engineering*, 46(4): 443–451.

Luo Haichao, 1989. Characteristics of fluvial processes and stability of the braided channel in the middle and lower reaches of the Yangtze River. *Journal of Hydraulic Engineering*, (6): 10–19. (in Chinese)

Mossa J, 2016. The changing geomorphology of the Atchafalaya River, Louisiana: A historical perspective. *Geomorphology*, 252: 112–127. doi: 10.1016/j.geomorph.2015.08.018.

Nanson R A, Nanson G C, Huang H Q, 2010. The hydraulic geometry of narrow and deep channels: Evidence for flow optimisation and controlled peatland growth. *Geomorphology*, 117(1/2): 143–154. doi: 10.1016/j.geomorph.2009.11.021.

Qian Ning, Zhang Ren, Zhou Zhide, 1987. River Bed Evolution. Beijing: Science Press, 127–140. (in Chinese)

Ramos Judith, Gracia Jesús, 2012. Spatial-temporal fluvial morphology analysis in the Quelite River: Its impact

on communication systems. *Journal of Hydrology*, 49(3): 432–433. doi: 10.1016/j.jhydrol.2011.05.007.

Regalla C, Kirby E, Fisher D *et al*., 2013. Active forearc shortening in Tohoku, Japan: Constraints on fault geometry from erosion rates and fluvial longitudinal profiles. *Geomorphology*, 195(4): 84–98. doi: 10.1016/j.geomorph.2013.04.029.

Schumm S A, 1985. Patterns of alluvial rivers. *Earth and Planetary Sciences*, 13(13): 5–27. doi: 10.1146/annurev.ea.13.050185.000253.

Schuurman F, Kleinhans M G, Middelkoop H, 2016. Network response to disturbances in large sand-bed braided rivers. *Earth Surface Dynamics*, 4(1): 25–45. doi: 10.5194/esurf-4-25-2016.

Schuurman F, Shimizu Y, Iwasaki T *et al*., 2015. Dynamic meandering in response to upstream perturbations and floodplain formation. *Geomorphology*, 253: 94–109.

Song X L, Xu G Q, Bai Y C *et al*., 2016. Experiments on the short-term development of sine-generated meandering rivers. *Journal of Hydro-environment Research*, 11: 42–58. doi: 10.1016/j.jher.2016.01.004.

Sun Zhaohua, Feng Qiufen, Han Jianqiao *et al*., 2013. Fluvial processes of sandbars in the junction reach of single-threaded channel to anabranching channel and its impact on navigation: A case study of the Tianxingzhou Reach of the Yangtze River. *Journal of Basic Science & Engineering*, 21(4): 647–655. (in Chinese)

Tang Jinwu, You Xingying, Hou Weiguo *et al*., 2015. Fluvial processes trend of Ma'anshan reach in Lower Yangtze River. *Journal of Sediment Research*, 67(1): 213–221. (in Chinese)

Wang Houjie, Yang Zousheng, Wang Yan *et al*., 2008. Reconstruction of sediment flux from the Changjiang (Yangtze River) to the sea since the 1860s. *Journal of Hydrology*, 349(3/4): 318–332.

Wang Suiji, Ni Jinren, Wang Guangqian, 2000. The evolution and direction of research in fluvial sedimentology. *Journal of Basic Science & Engineering*, 8(4): 362–369. (in Chinese)

Wohl E, 2015. Particle dynamics: The continuum of bedrock to alluvial river segments. *Geomorphology*, 241: 192–208. doi: 10.1016/j.geomorph.2015.04.014.

Xia Junqiang, Deng Shanshan, Lu Jinyou *et al*., 2016. Dynamic channel adjustments in the Jingjiang Reach of the Middle Yangtze River. *Scientific Reports*, 6: 22802.

Xu Jiongxin, 1997. Study of sedimentation zones in a large sand-bed braided river: An example from the Hanjiang River of China. *Geomorphology*, 21(2): 153–165. doi: 10.1016/S0169-555X(97)00039-1.

Yin Xueliang, 1965. A preliminary study on the formation cause of the bend river and the experiment of making riverbed. *Journal of Geographical Sciences*, 31(4): 287–303. (in Chinese)

You Xingying, Tang Jinwu, Zhang Xiaofeng *et al*., 2016. Preliminary study on the characteristics and origin of barrier river reach in the Middle and Lower Yangtze River. *Journal of Hydraulic Engineering*, 47(4): 545–551. (in Chinese)

Yu Wenchou, 1987. Action of nodes of the braided channel at the Lower Yangtze River in the fluvial processes. *Journal of Sediment Research*, (4): 12–20. (in Chinese)

Zhang Dujing, Sun Hanzhen, 1983. A preliminary study on the effect of the changes of the hydraulic conditions in bends on the river pattern of the upper and lower Jingjiang stretches of the Yangtze River. *Journal of Sediment Research*, 3(1): 14–24. (in Chinese)

Zhang Wei, Yang Yunping, Zhang Mingjin *et al*., 2017. Mechanisms of suspended sediment restoration and bed level compensation in downstream reaches of the Three Gorges Projects (TGP). *Journal of Geographical Sciences*, 27(4): 463-480.

Zhang Zhitang, Lin Wanquan, Shen Yongjian, 1984. An approach on the main current belt of stream flow in river bend. *Journal of Yangtze River Scientific Research Institute*, (1): 47–56. (in Chinese)